Applied Water Science (2021) 11:149
https://doi.org/10.1007/s13201-021-01481-7

ORIGINAL ARTICLE

Adsorption of chromium (Cr^{6+}) on dead biomass of *Salvinia molesta* (Kariba weed) and *Typha latifolia* (broadleaf cattail): isotherm, kinetic, and thermodynamic study

Asha Singh[1] · **Sunil Kumar**[1] · **Vishal Panghal**[1]

Received: 8 January 2021 / Accepted: 6 August 2021 / Published online: 14 August 2021

Abstract
This study evaluated the adsorption of Cr^{6+} from aqueous solution using dead biomass of aquatic plants *Salvinia molesta* (Kariba weed) and *Typha latifolia* (broadleaf cattail). The batch experiments were carried out to study the effects of pH, adsorbent dose, initial metal concentration, contact time, agitation speed in rotation per minute (rpm), and temperature. Fourier transform infrared spectroscopy (FTIR) and scanning electron microscopy (SEM) were used to characterize the adsorbent and analyze the functional groups and morphology of the adsorbent, respectively. The hydroxyl and amine groups were the main functional groups involved in the adsorption. Both adsorbents showed good results at pH 1, metal concentration of 20 mg/L for Cr^{6+} removal, and adsorption equilibrium was attained within 60 min with 150 rpm at 25 °C. The adsorption rate obtained was above 95% for both the adsorbents at a dose of 0.150 g for *S. molesta* and 0.8 g for *T. latifolia*. Isotherm and kinetic models were applied on the adsorption data. The monolayer adsorption capacity (q_m) was found to be 33.33 mg/g for *S. molesta* and 10.30 mg/g for *T. latifolia*. The Langmuir isotherm was better fitted to *S. molesta*, while the Freundlich isotherm was better fitted to *T. latifolia*. It was reported that the pseudo-second-order model ($R^2 = 0.999$) was better fitted to the adsorption data for both the adsorbents. The thermodynamic study was also conducted and found the adsorption process was exothermic and spontaneous. Results revealed the good adsorption potential of *S. molesta* and *T. latifolia*, and they can be used for the removal of hexavalent chromium.

Keywords Adsorption · Isotherm · Chromium · Adsorbent · Kinetics

Introduction

Chromium pollution is a serious problem of water resources that affects the health of the environment and human beings. The main sources of chromium discharge are anthropogenic sources like electroplating, pigment manufacturing, cement and steel industries, photography, leather tanning, and magnetic tapes, etc. (Flores-Cano et al. 2016; Babu and Gupta 2008). Chromium exists in two forms, Cr^{3+} and Cr^{6+}, and these are stable forms of chromium. Notably, Cr^{6+} is considered more harmful than Cr^{3+} while Cr^{3+} is an important essential trace metal for the metabolism of living beings. Cr^{6+} is also considered carcinogenic, mutagenic, toxic, and teratogenic (Wittbrodt and Palmer 1995). It is of main concern because it is very hazardous to human health. Its exposure to human beings causes skin irritation, liver damage, and gastrointestinal problems (Raji and Anirudhan 1998). Due to the ill effects of Cr^{6+} on human beings, it must be removed from effluents before discharging into water bodies which are the ultimate source of waste disposal.

Various techniques for chromium removal from wastewater have been employed, which include ion exchange, chemical precipitation, electrochemical reduction, membrane filtration, ultra-filtration, and adsorption (Grimshaw et al. 2011; Feng and Qi 2011; Oehmen et al. 2006; Liu et al. 2013; Llanos et al. 2010; Loganathan et al. 2018). Among all these, adsorption was found to be better than all these removal techniques. These techniques require high capital and operational costs, incomplete treatment, high energy, and chemical requirements and may be associated with the release of sludge and other waste products, which require safe disposal (Weis and Weis 2004). This needs a

✉ Sunil Kumar
sunilevs@yahoo.com

[1] Department of Environmental Sciences, Maharshi Dayanand University, Rohtak, Haryana 124001, India

cost-friendly and economically efficient method to remove the disadvantages of conventional methods. The process of adsorption was found to be more reliable and promising as it involves high efficiency of metal removal, local availability of adsorbents, simple operation, low capital cost, less sludge generation, the requirement of no additional nutrient, recovery of metal, and regeneration potential of the adsorbents (Kratochvil and Volesky 1998a; Musico et al. 2013; Thitame and Shukla 2017).

Adsorption is considered to be a simple, easy, and cost-friendly process for the removal of heavy metals by using adsorbents. Adsorption is the transfer of mass of a substance from the liquid phase onto the surface of a solid (adsorbent) that makes a molecular or atomic film (adsorbate). In earlier times, activated carbon was used as an effective adsorbent due to its large surface area, but its high cost makes the adsorption not cost-effective (Jianlong et al. 2000). This leads to the development of low-cost adsorbents from cheap and easily available materials that can be used in adsorption on a large scale. Various low-cost adsorbents, viz. fungi, algae, agricultural waste, peels of fruits, bagasse, industrial waste, sawdust, rice husk, and flower stalks including aquatic plant biomass, have been used for the removal of various heavy metals (Ahluwalia and Goyal 2007; Afroze and Sen 2018; Ali et al. 2016; Jain et al. 2010; Hashem et al. 2020).

S. molesta is a floating fern which grows on slow-moving fresh water and grows rapidly like a dense mat on the surface of river, lake, and ponds. It is also listed in the UN list of the world's worst invasive species. They chock the water flow, decrease the light, and lower oxygen in the water which leads to the disturbance in the water ecosystem. *T. latifolia* (common name cattail) has rapid growth, easily available nearby water bodies. They help in keeping a lake healthy by removing the runoffs but often become a nuisance also by forming dense rhizome mats and litter which has an impact on aquatic systems. The dense growth of *T. latifolia* may affect other plants also to establish or survive. This study evaluates the possibility of these aquatic plants to be used as adsorbents for Cr^{6+} removal. As per the literature, there is few work related to the use of these species for the adsorption. *S. molesta* has also been used in adsorption of phenol and adsorption capacity found was 100.12 mg/g at pH 6 and 40 °C (Sankaran and Anirudhan 1999). Similarly *T. latifolia* was used as an adsorbent for the removal of pesticides (Tolcha et al. 2020) and root powder for removal of Cu^{2+}(37.35 mg/g) and Zn^{2+}(28.80 mg/g) within 60 min (Rajaei et al. 2013). The batch experiments were carried out by varying different parameters like pH, contact time, adsorbent dose, agitation speed, initial metal concentration, and temperature to study equilibrium, isotherm, kinetic, and thermodynamics of adsorption data. SEM and FTIR analysis were also done for adsorbent characterization and to study the structure of adsorbent and functional groups involved in the adsorption.

Materials and methods

Reagents and apparatus

All chemicals used were of pure analytical grade during the experiments. The solution of chromium was made by dissolving an appropriate amount of potassium dichromate $K_2Cr_2O_7$ in double-distilled water and used in adsorption process. The solution of 1,5-diphenylcarbazide was made by dissolving 250 mg in 50 mL acetone. The pH was measured using a pH meter. UV–Vis spectrophotometer was used for the analysis of initial and final Cr^{6+} ion concentrations.

Preparation of adsorbent

The aquatic plants *S. molesta* (whole plant) and *T. latifolia* (whole plant except root and flower) were collected from Bhindawas lake (76°32′30″ E; 28°32′36″ N) Jhajjar, Haryana, India. The plants were carried to the laboratory and rinsed with de-ionized water several times to remove dirt and impurities (Ahmad and Haseeb 2015). The aquatic plants were identified from the botany department of the University. These plants were initially dried under sunlight for 12 h and then dried in an oven for 72 h at 60 °C. The dried biomass was powdered by the grinder and sieved through a 60-mesh screen and used as adsorbent.

Characterization of adsorbent

The surface structure of the adsorbent was analyzed using SEM (EVO 18 Zeiss, SAIF, AIIMS, Delhi), before and after the adsorption. The determination of functional groups involved in the adsorption was done using FTIR (Bruker Alpha, Genetics Department, MDU) spectrometer in the wavenumber region of 400–4000 cm^{-1} before and after the adsorption of Cr^{6+} on the surface of the adsorbent.

Batch experiment

The stock solution (1000 mg/L) of chromium was made by dissolving an appropriate amount of potassium dichromate $K_2Cr_2O_7$ in double-distilled water. After that, standard solutions of different concentrations were made using the stock solution. The batch experiments were done with 100 ml of chromium solution in 250-ml conical flasks. The solutions of 1 N H_2SO_4 and 1 N NaOH were used for adjusting the pH of the metal solution before adding the adsorbent. The effect of pH, adsorbent dose, initial metal concentration, contact time, agitation speed, and temperature was assessed in batch experiments (Singh et al. 2019). The conical flasks having 0.1 g dose of adsorbent with 100 ml of Cr^{6+} solution were agitated in an incubator shaker at 25 °C with 150 rpm for 60 min for pH

optimization. After that, adsorbent was separated using Whatman filter paper. The concentration of Cr^{6+} in synthetic solution was determined by using UV–Visible spectrophotometer (UV 3000 series) at 540 nm by reacting it with 1, 5-diphenyl carbazide giving red-violet color in an acidic medium as a complex agent (APHA 1985). The experiments were carried out in triplicates at different pH values from 1 to 8 for Cr solution, adsorbent dose ranges from 0.025 to 0.250 g for adsorbent *S. molesta* and 0.1 to 0.8 g for adsorbent *T. latifolia*, initial metal concentration from 20 to 80 mg/L for Cr^{6+}, contact time from 15 to 120 min, agitation speed from 50 to 250 rpm, and temperature ranges from 15 to 55 °C. The amount of Cr^{6+} adsorbed per unit mass of adsorbent at equilibrium as adsorption capacity q_e (mg/g) was calculated using Eq. (1).

$$q_e = \frac{(C_i - C_e)\,V}{x} \tag{1}$$

where q_e is the amount of metal adsorbed at equilibrium (mg/L), C_i and C_e are the initial and equilibrium concentrations of the Cr^{6+} metal (mg/L), V is the volume of the metal solution (L), and x is the weight of the adsorbent (g). The removal efficiency of Cr^{6+} metal on the adsorbent was calculated using Eq. (2).

$$\text{Removal}(\%) = \frac{(C_i - C_e)}{C_i} \times 100 \tag{2}$$

where C_i is initial and C_e is the equilibrium concentration of the Cr^{6+} metal (mg/L).

Isotherm, kinetics, and thermodynamic studies

The isotherm models, namely Freundlich, Langmuir, and Temkin isotherms, were applied on the adsorption data. The sorption mechanism types were given by kinetics study. Lagergren's pseudo-first-order and pseudo-second-order equations predict the adsorption kinetics. The intraparticle diffusion is a secondary process and evaluated adsorption capacity with the square root of time, which determines the adsorption of adsorbate on any porous material. The thermodynamic parameters, enthalpy ($\Delta H°$), entropy ($\Delta S°$), and free energy ($\Delta G°$) for sorption of Cr^{6+} on *S. molesta* and *T. latifolia* were determined from temperature-dependent data.

Results and discussion

Characterization of adsorbent

FTIR analysis

FTIR results for unloaded and loaded adsorbent *S. molesta* are shown in Fig. 1a, b, respectively. The significant peaks were observed at approximately 3291, 2917, 1603, 1374, and 1032 cm^{-1}. The Cr ion-free spectrum of *S. molesta* shows an absorption peak at 3291, 2917, and 1603 cm^{-1} representing –OH stretching, C-H stretching alkane, N–H bending of amine peaks, respectively. A peak at 1032 cm^{-1} corresponds to C-N stretching in amine, and a peak at 1374 cm^{-1} represents O–H bending in phenol. Other small peaks were observed at 2849, 1451, 1316, 666, 630, and 617 cm^{-1}. It was observed that peak form in FTIR spectra did not change so much after Cr^{6+} adsorption and indicated that metal Cr does not cause any significant change in the basic chemical composition of adsorbents. A stretching band observed in the range 1000–1460 cm^{-1} may be corresponding to the C-O bond in alcohols, carboxylic acids, phenols, or esters (Borah et al. 2012). The peaks at 3291, 2917, 1603, 1415, 1252, 1032, and 666 cm^{-1} had shifted, respectively, to 3281, 2916, 1592, 1418, 1261, 1024, and 664 cm^{-1}. The shift and reduction of peaks at 3291, 1603, and 1032 cm^{-1} were mainly due to hydroxyl and amine groups in *S. molesta* adsorbent.

For *T. latifolia* adsorbent, FTIR spectra before and after adsorption are shown in Fig. 1c, d, respectively. The significant peaks were observed at 3326, 2918, 1729, 1602, 1371, 1241, and 1033 cm^{-1} for unloaded *T. latifolia* adsorbent. The broad O–H band at 3326 cm^{-1} had shifted to 3314 cm^{-1} revealed the possible involvement of the hydroxyl group (–OH stretching). The peaks at 2832, and 1315 cm^{-1} had shifted, respectively, at 2860, and 1318 cm^{-1} showed the involvement of N–H stretching of the amine group and O–H bending of phenol. The peak at 2918 corresponds to stretching vibrations of the C-H groups (Goswami et al. 2014). Other peaks at 2918, 2151, 1729, 1425, and 662 cm^{-1} were shifted, respectively, at 2916, 2045, 1725, 1422, and 666 cm^{-1}. The hydroxyl and amine groups were the main functional groups involved in the adsorption. Some similar results were obtained by different investigators (Meitei and Prasad 2014; Li et al. 2016).

SEM analysis

Figure 2a, b shows the SEM images of the adsorbent *S. molesta* before and after adsorption, respectively. The particles did present clear crystals, and the surface was so irregular. The surface adsorbed Cr^{6+} ions as biomass has a porous structure with a large surface area which was suitable for adsorption. Similarly, Fig. 2c, d is the SEM images of adsorbent *T. latifolia* before and after loading of Cr^{6+} ions. It was clear from the images that the adsorbent surface had long elongated cylindrical structures with surface area and favors adsorption of Cr^{6+} on its surface.

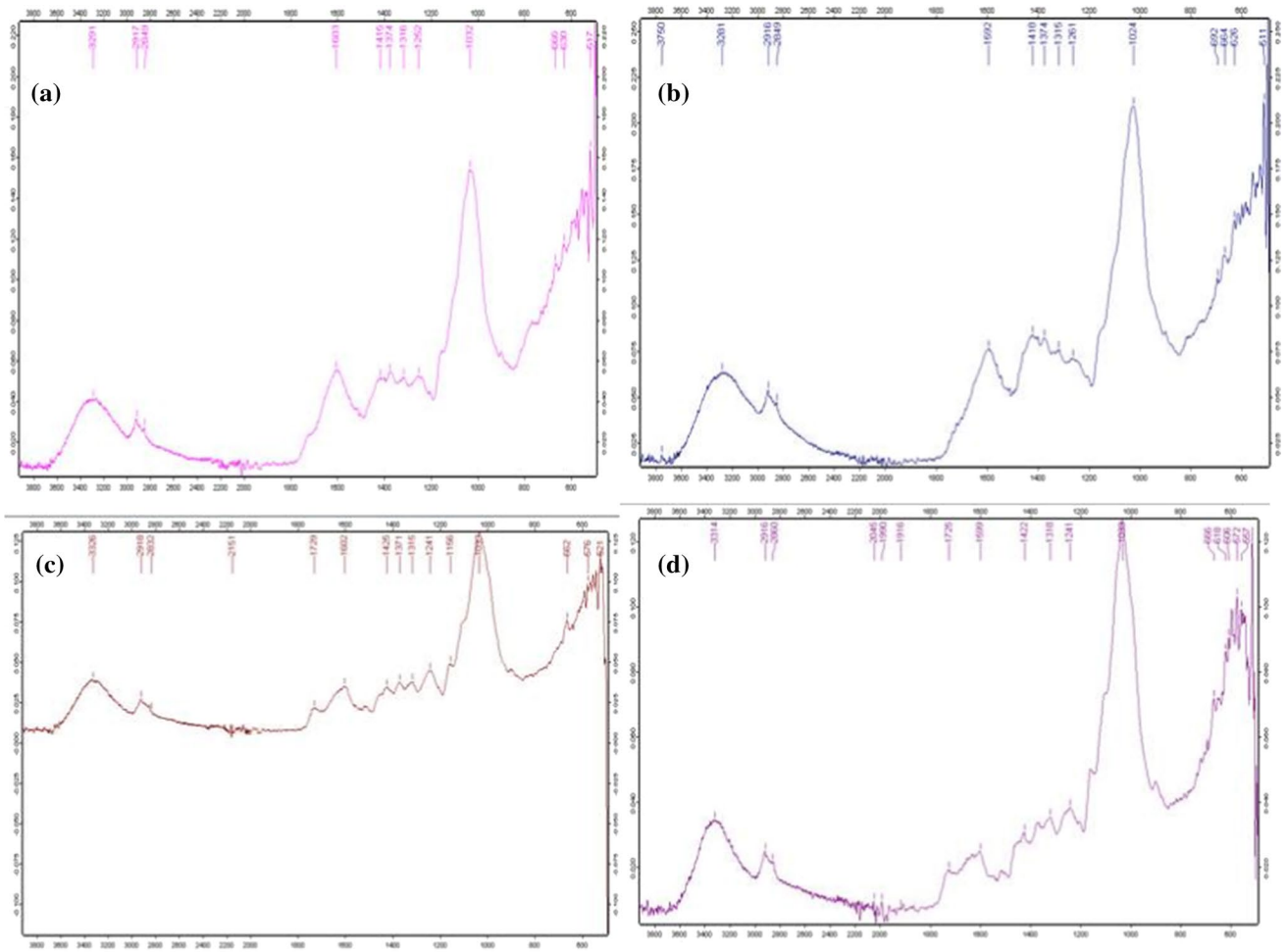

Fig. 1 FTIR spectra of unloaded **a** and loaded **b** *S. molesta* and unloaded (c) and loaded (d) *T. latifolia*

Batch experiment

In adsorption, a layer of adsorbate is formed on the surface of the adsorbent. It can be both physical and chemical processes. In physical adsorption, due to imbalance in surface forces, adsorbate molecules in the solution form a surface layer on adsorbent when in contact with solid surface and it resulted from molecular condensation in the capillaries of the solid. In chemical adsorption, the molecular layer of adsorbate on the surface is formed through chemical interaction. High molecular weighted substances can be easily adsorbed on the surface. So, heavy metals are removed from wastewater through the process of adsorption by making a layer on the surface of the adsorbent (Sharma et al. 2016). The cellulosic content in plant-based adsorbent shows higher metal binding capacity due to presence of polyfunctional metal binding sites for both cation and anions (Patel 2012). Various factors like pH, adsorbent dose, contact time, adsorbate concentration, and temperature also affect the rate of adsorption and also need to be optimized.

Effect of pH

The pH has an important role in the adsorption of Cr^{6+} ions. The adsorption experiment was carried out in the pH range of 1 to 8 at an interval of 1 for Cr^{6+}, adsorbent dose of 0.1 g, initial metal concentration of 20 mg/L, a contact time of 60 min with an agitation speed of 150 rpm at 25 °C for both the adsorbents *S. molesta* and *T. latifolia*. The effect of pH on Cr^{6+} removal by both the adsorbents is shown in Fig. 3. It was observed that both adsorbents gave maximum removal of Cr^{6+} at pH 1, and after that, adsorption percentage decreases as pH increases. A similar trend was followed by adsorption capacity (q_e). The cell wall of the adsorbent may have a large number of functional groups and the pH dependence of the metal adsorption may often be related to the type, ionic state, and metal chemistry of these functional groups in solution (Chen et al. 2002). The dominant form of Cr^{6+} is $HCrO_4^-$ at low pH which arises from the hydrolysis of $Cr_2O_7^{2-}$ according to the equation (Jain et al. 2009):

$$Cr_2O_7^{2-} + H_2O = 2HCrO_4^-$$

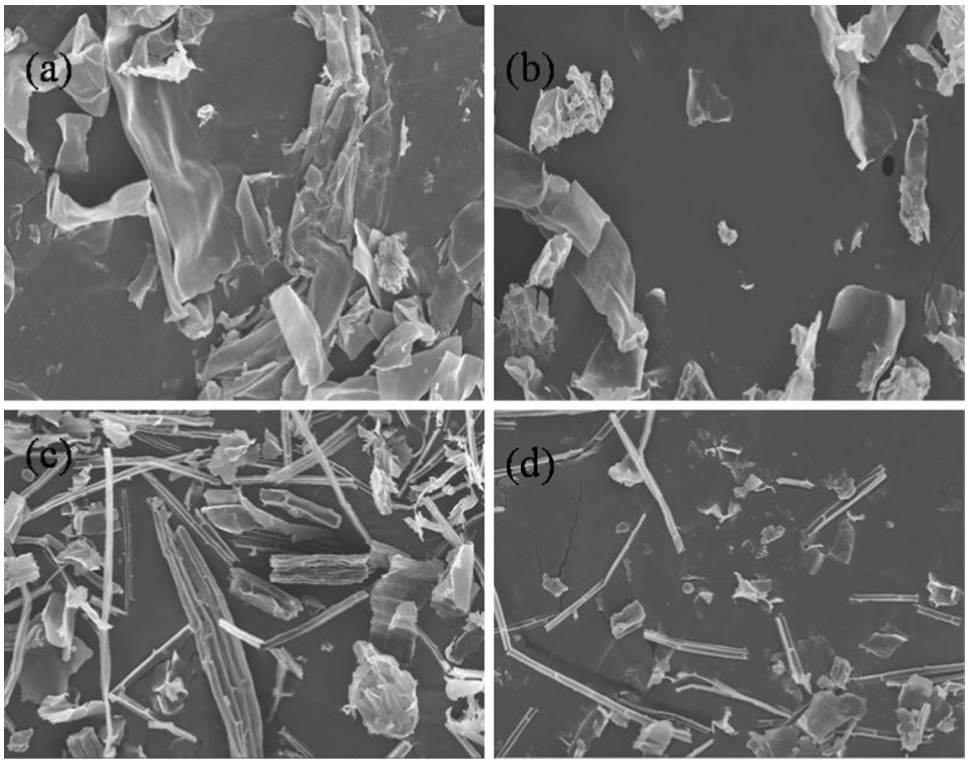

Fig. 2 SEM images (a) before, and (b) after adsorption on *S. molesta*, (c) before, and (d) after adsorption on *T. latifolia*

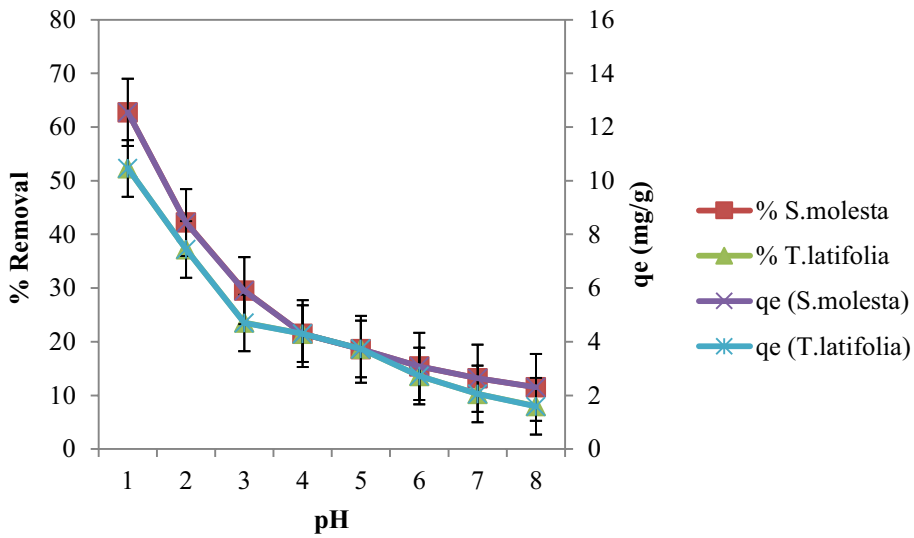

Fig. 3 Effect of pH on Cr^{6+} adsorption by *S. molesta* and *T. Latifolia*

Cr^{6+} exists in the form of $HCrO_4^-$ at acidic pH, as pH increases, it starts changing into its other forms CrO_4^{2-} and $Cr_2O_7^{2-}$. Decreased adsorption of Cr^{6+} with increase in pH value may be due to the dual competition of two anions (CrO_4^{2-} and OH^-) adsorbed on the surface of the OH^-dominated adsorbent (Bayat 2002; Gupta and Babu 2009). A similar trend was also obtained by using *Eichhornia crassipes* for the adsorption of Cr^{6+} (Mohanty et al. 2006; Saraswat and Rai 2010).

Effect of adsorbent dose

Adsorption experiments were carried out at different doses (0.025, 0.050, 0.075, 0.1, 0.125, 0.150, 0.175, 0.2, 0.225, 0.250 g) for *S. molesta* and (0.1, 0.2, 0.3, 0.4, 0.5, 0.6, 0.7, 0.8 g) for *T. latifolia* at 20 mg/L of Cr solution, pH 1, contact time of 60 min with 150 rpm at 25 °C to assess the adsorption of Cr^{6+} ions. The effect of dose on the adsorption of Cr^{6+} by *S. molesta* and *T. latifolia*

is shown in Figs. 4 and 5, respectively. It was observed that the adsorption percentage of Cr^{6+} increases with increase in adsorbent dose and becomes saturated. The Cr^{6+} removal increased from 35.2 to 95.3% with increase in dose from 0.025 to 0.25 g and found equilibrium adsorption of 95.3% at 0.150 g of dose for *S. molesta*. In the case of *T. latifolia,* the percentage removal of Cr^{6+} increased from 41.3 to 95.1% with increase in doses from 0.1 to 1 g. While q_e decreases, the adsorbent dose increases. This may be due to the increase in surface area for adsorption of metal ions with increase in dose and thus increases more availability of binding sites/functional groups for adsorption (Meitei and Prasad 2014; Afroze and Sen 2018). Similar results for Cr^{6+} removal using *Eichhornia crassipes* (Mohanty et al. 2006), *Pistia stratiotes* (Lima et al. 2013) were observed.

Effect of initial metal concentration

The effect of initial metal concentration was determined by conducting the experiments by varying the concentration (20, 30, 40, 50, 60, 70, 80 mg/L) of metal solution at pH 1, an adsorbent dosage of 0.150 g for *S. molesta* and 0.8 g for *T. latifolia,* contact time 60 min with 150 rpm at 25 °C. The effect of initial metal concentration on the removal of Cr^{6+} by both the adsorbents is shown in Fig. 6. It was seen from the graph that adsorption efficiency was maximum at 20 mg/L, and after that, it decreases with an increase in the concentration of Cr solution. Both adsorbents showed more than 95% removal at 20 mg/L of chromium solution. This may be due to the saturation of adsorption sites on adsorbent at higher ionic concentrations (Al-Senani and Al-Fawzan

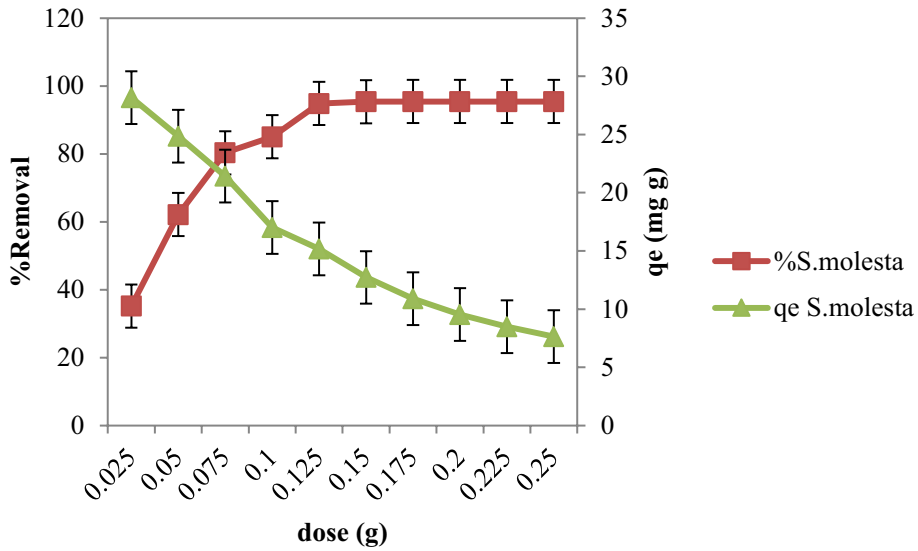

Fig. 4 Effect of adsorbent dose on Cr^{6+} adsorption by *S. molesta*

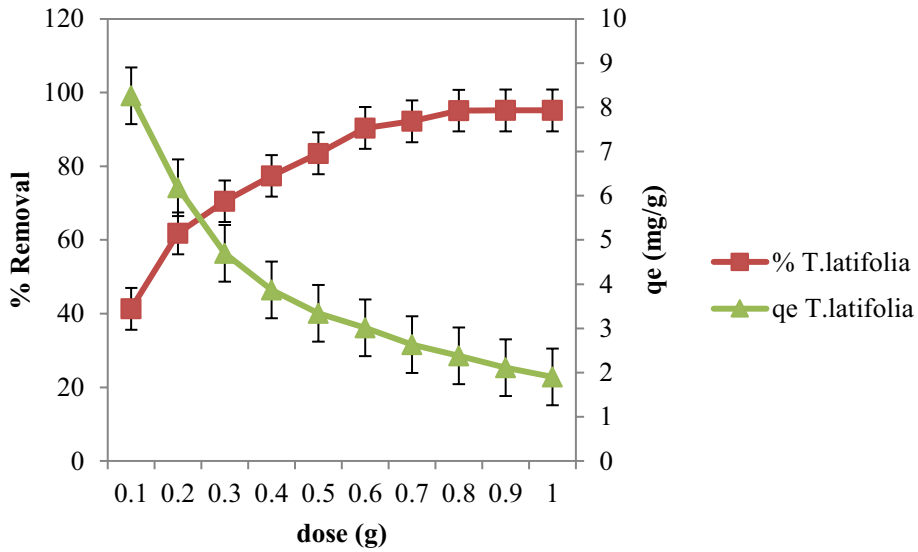

Fig. 5 Effect of adsorbent dose on Cr^{6+} adsorption by *T. latifolia*

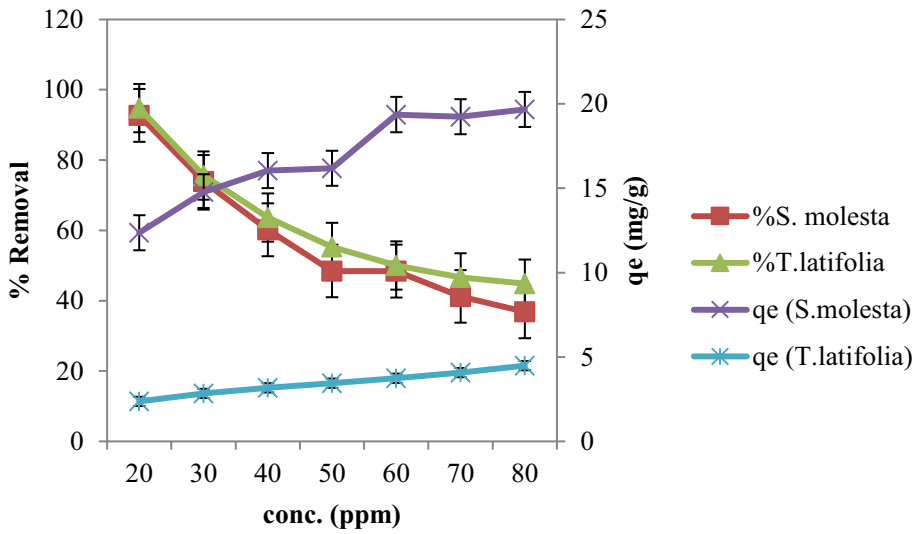

Fig. 6 Effect of initial metal concentration on Cr^{6+} adsorption by *S. molesta* and *T. Latifolia*

2018). The initial concentration of metal ions provides the driving force to overcome the mass transfer resistance of the adsorbate between the aqueous and the solid phase. At low concentrations, adsorption increases as adsorption sites become more available for faster adsorbate binding and make the process faster, but at higher concentrations, the adsorbate must spread over the sorbent surface by intraparticle diffusion (Afroze et al. 2015). On the other hand, q_e increases on increasing metal concentration as more active binding sites were available for adsorption. Other investigators also studied similar results using other adsorbents like *Eichhornia crassipes* and *Lemna minor* (Hassoon and Najem 2017; Balasubramanian et al. 2019), Alligator weed (Wang et al. 2008).

Effect of contact time

The time has a significant effect on the adsorption of Cr^{6+}. The effect of time on the removal of Cr^{6+} using both adsorbents *S. molesta* and *T. latifolia* is shown in Fig. 7. The experiments were carried out at various contact times (15, 30, 45, 60, 75, 90, 105, 120 min), pH 1, the concentration of 20 mg/L with 150 rpm at 25 °C. The results showed an increase in adsorption rate as well as adsorption capacity (q_e) of Cr^{6+} with an increase in contact time from 15 to 60 min for both the adsorbents, and after that, there is no significant adsorption beyond 60 min. This may be due to the saturation of adsorption sites on the surface of the adsorbent with an increase in time as the biomass has fixed active sites

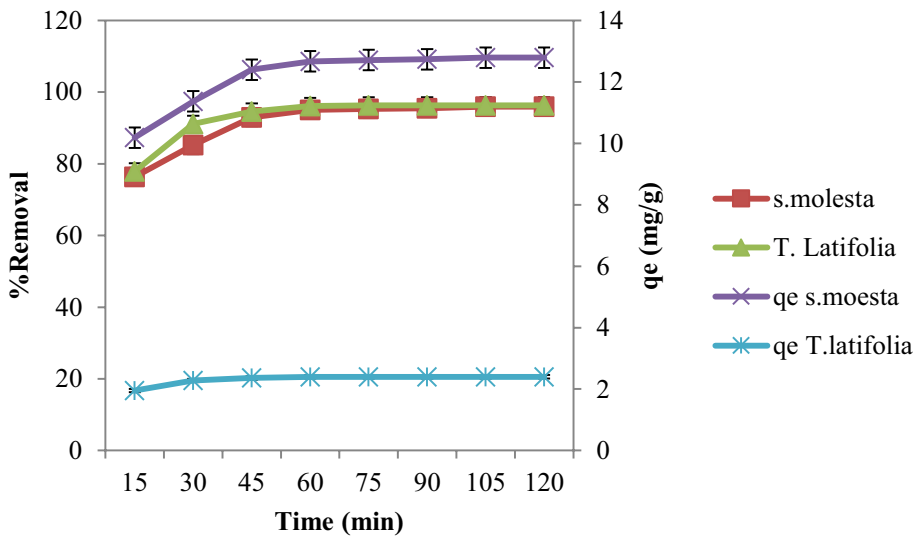

Fig. 7 Effect of time on Cr^{6+} adsorption by *S. molesta* and *T. Latifolia*

for adsorption (Hassoon and Najem 2017). Similar results were obtained by using *Lepironia articulata* (Kaewsichan and Tohdee 2019), *Pistia stratiotes* (Das et al. 2013), and *Hydrilla verticillata* (Bind et al. 2018).

Effect of agitation speed

The effect of agitation speed in rpm on adsorption of Cr^{6+} by both the adsorbents *S. molesta* and *T. latifolia* is shown in Fig. 8. The effect of agitation speed was studied by varying rpm (50, 100, 150, 200, 250) at pH 1, the concentration of 20 mg/L, contact time of 60 min at 25 °C by taking optimized doses for both the adsorbents. The adsorption rate and q_e increase with increase in rpm and reach equilibrium at 150 rpm, and after that, there was no significant increase in the adsorption. This may be due to the reduction in the thickness of the boundary layer around the adsorbent particles (Hanafiah et al. 2009). A higher shaking rate promoted the transfer of Cr^{6+} ions from the total solution to the surface of the adsorbent and shortened the equilibrium time for adsorption. A similar finding was obtained in the adsorption of Cr^{6+} using *Pistia stratiotes* (Das et al. 2013).

Effect of temperature

Temperature also plays an important role in adsorption. Experiments were performed at various temperatures (15, 25, 35 45, 55 °C) with pH 1, a contact time of 60 min, a metal concentration of 20 mg/L, and agitation speed of 150 rpm by taking optimized doses for both the adsorbents. The effect of temperature on the adsorption of Cr^{6+} is shown in Fig. 9. The adsorption percentage as well as adsorption capacity (q_e) increased with an increase in temperature and got reduced after 35 °C. The Cr^{6+} removal % increased from 67.75 to 95.1% (*S. molesta*) and 71.2 to 94.8% (*T. latifolia*) with increase in temperature from 15 to 35 °C and after that decreases. The adsorption sites with low activation energy were occupied at low temperatures, while high activation energy could be occupied at higher temperatures. A similar result was observed by Tewari et al. (2005), where they obtained a maximum adsorption capacity of Cr^{6+} at 55 °C onto *M. hiemalis*. At higher temperatures, a decrease in the percentage of the adsorption may be due to an increase in the thermal energy, which induces greater movement of the adsorbate causing a decrease in adsorption (Wanees et al. 2013).

Isotherm and kinetic study

Adsorption isotherms

The equilibrium relationship between adsorbent and adsorbate (metal ions) in the solution was illustrated using isotherm models, Langmuir, Freundlich, and Temkin. The isotherm studies were performed by varying adsorbent dosage at pH 1, initial concentration of 20 mg/L for 1 h agitation time, at 25 °C with 150 rpm agitation speed.

The **Langmuir** isotherm is based on the assumption that monolayer adsorption takes place on a homogeneous surface by uptake of metal ions without any interaction between the adsorbed ions (Langmuir 1918).

The linear form of the equation is described as:

$$\frac{C_e}{q_e} = \frac{1}{bq_m} + \frac{C_e}{q_m} \tag{3}$$

where q_e is the metal adsorption capacity at equilibrium (mg/g), C_e is the metal concentration at equilibrium (mg/L).

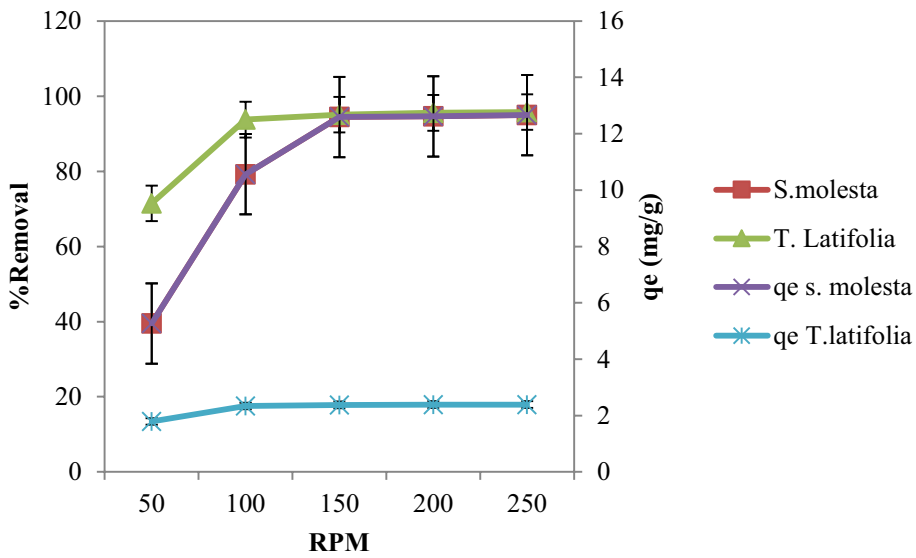

Fig. 8 Effect of agitation speed (rpm) on Cr^{6+} adsorption by *S. molesta* and *T. Latifolia*

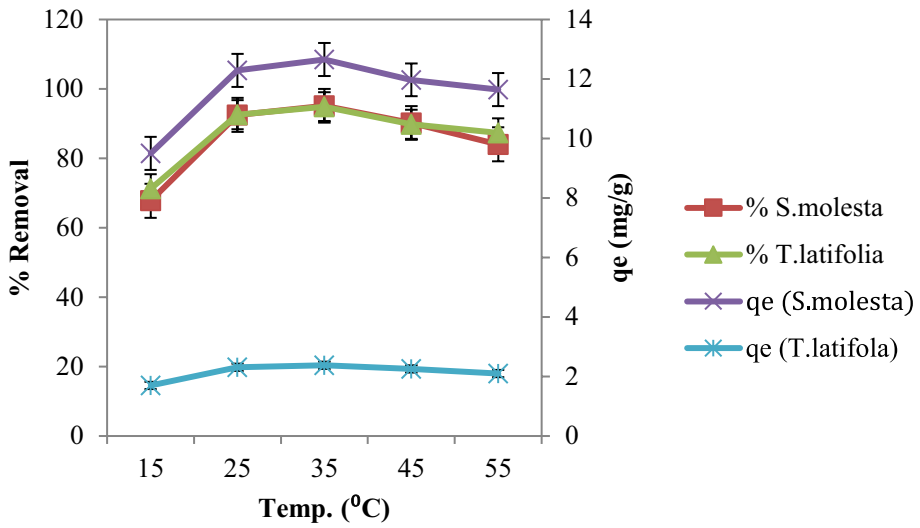

Fig. 9 Effect of temperature on Cr^{6+} adsorption by *S. molesta* and *T. latifolia*

q_m is the maximum adsorption capacity (mg/g), and b is the equilibrium Langmuir constant. The values of b and q_m were calculated using slopes and intercepts, respectively, from the plot of C_e/q_e vs C_e.

A dimensionless constant called separation factor (R_L) was calculated from Langmuir describing the essential characteristics of the isotherm.

Separation factor

$$R_L = \frac{1}{(1 + bC_i)} \tag{4}$$

where R_L is a dimensionless constant called separation factor, b is the Langmuir equilibrium constant, and C_i is the initial concentration of the metal ion. There are four possibilities for the value of R_L: $0 < R_L < 1$ for favorable adsorption, $R_L > 1$ for unfavorable adsorption, $R_L = 1$ for linear adsorption, and $R_L = 0$ for irreversible adsorption.

From Fig. 10 and Table 1, the correlation coefficient values (R^2) obtained were 0.980 and 0.831 for adsorbents *S. molesta* and *T. latifolia*, respectively. The value of R^2 for *S. molesta* favors the Langmuir isotherm while showing the unfitness to the equilibrium data for *T. latifolia*. The separation factors (R_L) using Eq. (4) obtained were 0.098 (*S. molesta*) and 0.2 (*T. latifolia*), which fell within the range, $0 < R_L < 1$, showing the feasibility of the adsorption process at all metal concentrations investigated. Langmuir isotherm fits adsorption data indicate monolayer adsorption (Soni and Padmaja 2014).

In **Freundlich** isotherm, molecules were adsorbed on the heterogeneous surfaces forming more than one layer with interactions occurring between the adsorbed molecules (Freundlich 1906).

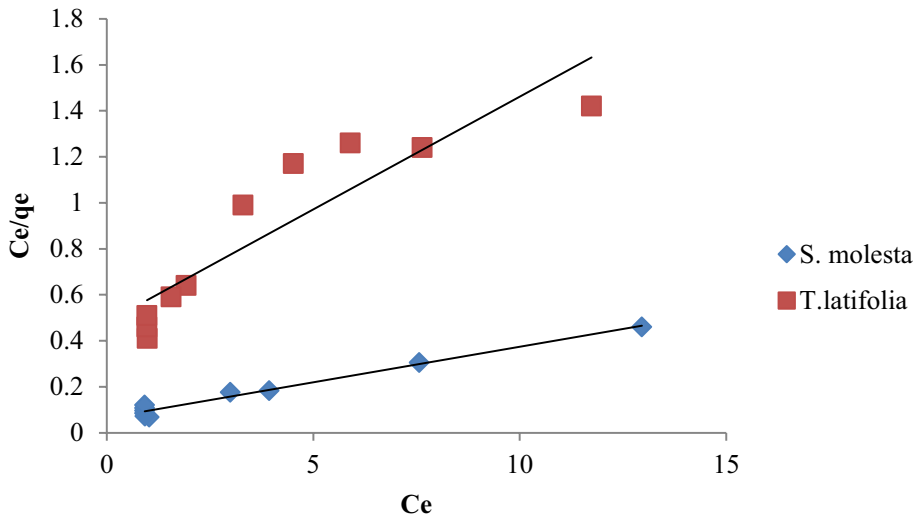

Fig. 10 Langmuir isotherm plot for Cr^{6+} adsorption on *S. molesta* and *T. latifolia*

Table 1 Comparison of isotherm parameters for adsorption of Cr^{6+} on *S. molesta* and *T. latifolia*

Isotherm model	Parameters	*Molesta*	*Latifolia*
Langmuir	q_m (mg/g)	33.33	10.30
	b	0.46	0.20
	R^2	0.980	0.830
	R_L	0.098	0.2
Freundlich	n	2.45	1.99
	K_F (L/g)	10.81	2.08
	R^2	0.829	0.953
Temkin	B_T (KJ/mol)	0.367	1.215
	A_T (g/L)	1.92	2.39
	R^2	0.920	0.864

The linear form of the equation is described as:

$$\log qe = \log K_F + \frac{1}{n}\log C_e \tag{5}$$

where C_e (mg/L) is the equilibrium concentration, q_e is the amount of metal ion adsorbed at equilibrium (mg/g), K_F indicates the adsorption capacity, and n represents the intensity of adsorption and these K_F and n can be obtained from the intercepts and slopes of the curve plotted between log C_e vs log q_e.

It was observed from Fig. 11 and Table 1 that the correlation coefficient values (R^2) obtained were 0.829 and 0.953 for adsorbents *S. molesta* and *T. latifolia*, respectively. The value of n was greater than 1 which favors the adsorption process. For *T. latifolia*, Freundlich isotherm is much more suited as the R^2 value is 0.953 higher than *S. molesta*.

The **Temkin** model was proposed by Temkin and Pyzhev (1940) to study the adsorption system. The Temkin model assumes that the heat of sorption linearly decreases rather than logarithmically with temperature. It can be expressed as:

$$q_e = \frac{RT}{B_T} lnA_T + \frac{RT}{B_T} lnC_e \tag{6}$$

where C_e is the metal concentration at equilibrium (mg/L), q_e is the amount of adsorbate adsorbed on adsorbent at equilibrium (mg/g), T is the absolute temperature (K), and R is gas constant (8.314 J/mol/K). B_T is the Temkin constant related to the heat of adsorption (J/mol), and A_T is the Temkin isotherm constant (g/L). The plot for Temkin was plotted between q_e vs ln C_e as shown in Fig. 12 for *S. molesta* and *T. latifolia*. The values of B_T and A_T can be calculated from the slopes and intercepts, respectively.

The value of the Temkin constant (B_T) signifies the nature of adsorption. When the value of B_T is less than 20 kJ/mol, it signifies physisorption. The Temkin constant (B_T) values obtained were 0.36 and 1.21 kJ/mol for adsorbent *S. molesta* and *T. latifolia*, respectively. It favors the physical sorption and R^2 values obtained were 0.920 and 0.864 for *S. molesta* and *T. latifolia*, respectively. The Temkin study showed the process was physical adsorption.

Adsorption kinetics

For determination of the adsorption rate, kinetic models, pseudo-first-order, pseudo-second-order, and intraparticle diffusion was studied for the adsorption data.

The pseudo-first-order kinetic equation or Lagergren model that describes the solute adsorption on adsorbent is given as (Lagergren 1898):

$$\log (q_e - q_t) = \log q_e - \frac{K_1 t}{2.303} \tag{7}$$

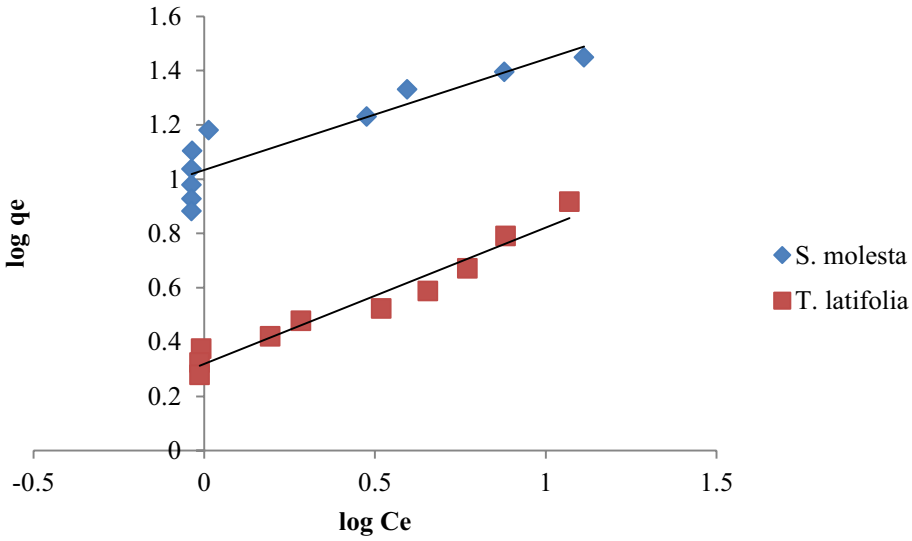

Fig. 11 Freundlich isotherm plot for Cr^{6+} adsorption on *S. molesta* and *T. latifolia*

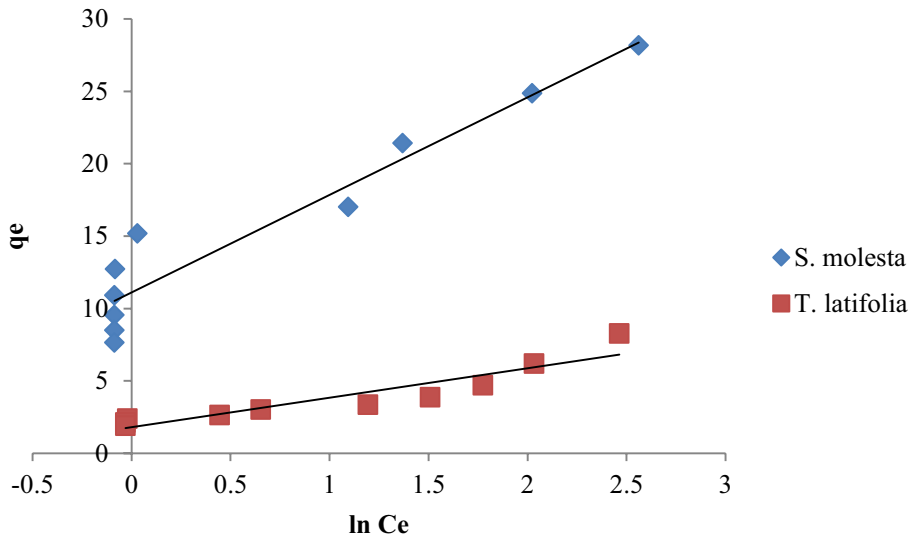

Fig. 12 Temkin plot for Cr^{6+} adsorption on *S. molesta* and *T. latifolia*

where q_e is equilibrium adsorption capacity (mg/g), q_t is the adsorption capacity at time t (min), and K_1 is the rate constant (1/min).

Kinetic plot for pseudo-first order was plotted between log (q_e–q_t) and t as shown in Fig. 13 for both the adsorbents. From the plot, values of K_1 and q_e were calculated by the slopes and intercepts, respectively. The correlation coefficients (R^2) obtained from Fig. 13 were 0.945 for *S. molesta* and 0.999 for *T. latifolia*. The correlation coefficient values are more than 0.9, suggesting good agreement between experimental and calculated adsorption capacities (Table 2).

The pseudo-second order in its linear form is represented as (Ho and Mckay 1999):

$$\frac{t}{q_t} = \frac{1}{K_2 q_e^2} + \frac{t}{q_e} \quad (8)$$

where q_e is equilibrium adsorption capacity (mg/g) and q_t is the adsorption capacity at time t (min). K_2 is the equilibrium rate constant (g/mg/min).

A pseudo-second-order kinetic curve was plotted between t/q_t and t as shown in Fig. 14. The values of q_e and K_2 were calculated by slopes and intercepts of the plot t/q_t vs t, respectively. The values of R^2 obtained were 0.999 for both the adsorbents. It was clear from Table 2 that there is a good agreement between calculated q_e and experimental q_{exp}. It showed that pseudo-second order was better fitted to the adsorption data.

The intraparticle diffusion model is based on the pore diffusion and intraparticle uptake in the adsorption. According to this, intraparticle diffusion of adsorbate varies proportionately with half power of time in adsorption and linearly represented by Weber and Morris (1963) to identify the diffusion mechanism:

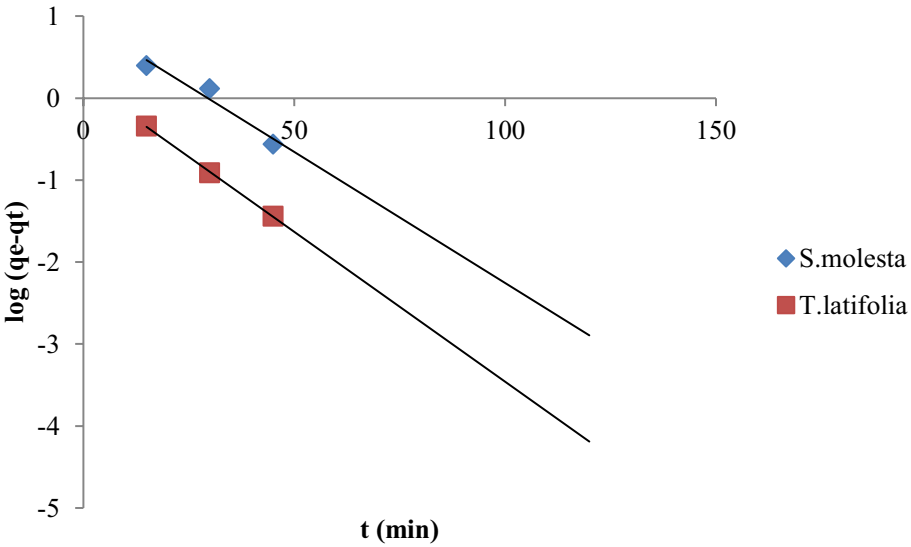

Fig. 13 Pseudo-first-order kinetic plot for Cr^{6+} adsorption on *S. molesta* and *T. Latifolia*

Table 2 Comparison of kinetic parameters for both adsorbents

Kinetic model	Parameters	*Salvinia molesta*	*Typha latifolia*
Experimental adsorption capacity	q_{exp} (mg/g)	12.66	2.4
Pseudo-first order	q_e (mg/g)	1.07	1.08
	K_1 (1/min)	2.16	0.45
	R^2	0.945	0.999
Pseudo-second order	q_e (mg/g)	13.33	2.46
	K_2 (g/mg/min)	0.018	0.153
	R^2	0.999	0.999
Intraparticle diffusion	k_i (mg/g min$^{0.5}$)	0.282	0.051
	x_i (mg/g)	10.05	1.915
	R^2	0.815	0.646

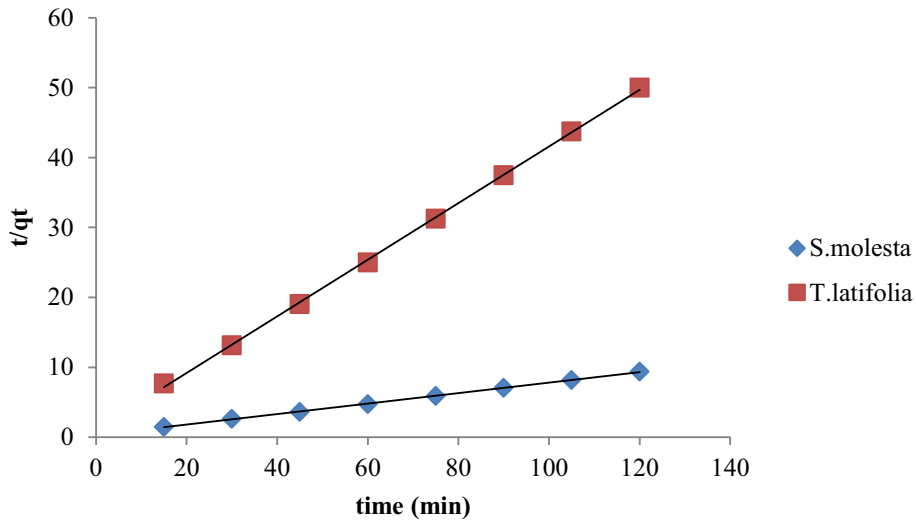

Fig. 14 Pseudo-second-order kinetic plot for Cr^{6+} adsorption on *S. molesta* and *T. latifolia*

$$q_t = k_i\sqrt{t} + x_i \tag{9}$$

where x_i shows the boundary layer thickness (mg/g), and k_i is the intraparticle diffusion rate constant (mg/g min$^{0.5}$). A plot between q_t and $\sqrt{t}$ was plotted for the intraparticle diffusion model (Fig. 15) to calculate the values of x_i and k_i from the intercepts and slopes, respectively. The boundary layer effect depends on the higher value of x_i (Singh and Bhateria 2020) as indicated in Table 2. The values of x_i obtained were 10.05 and 1.915 mg/g for *S. molesta* and *T. latifolia*, respectively.

From the kinetic results, it was observed that the pseudo-second-order kinetic model was better fitted to the adsorption data as compared to the pseudo-first-order kinetic model.

Thermodynamic study

The thermodynamic parameters like enthalpy ($\Delta H°$), free Gibb's energy ($\Delta G°$), and entropy ($\Delta S°$) variation control the spontaneity of an adsorption process. If $\Delta G°$ decreases with increase in temperature, then the adsorption process is said to be spontaneous (Ngah and Hanafiah 2008). The thermodynamic study was carried out at different temperatures 298, 308, 318, and 328 K. The thermodynamic parameters were determined using the following equations:

$$\ln K_d = \frac{\Delta S^{\circ}}{R} - \frac{\Delta H^{\circ}}{RT} \tag{10}$$

$$\Delta G° = \Delta H° - T\Delta S° \tag{11}$$

where $K_d = q_e/C_e$ is the equilibrium constant, q_e is the adsorption capacity of Cr^{6+} at equilibrium (mg/g), Ce is the equilibrium concentration of Cr^{6+} solution (mg/L), T is the temperature (K), and R is the gas constant (8.314 J /mol/K). The thermodynamic parameters enthalpy ΔH° (kJ/mol) and entropy ΔS° (kJ/K. mol) were calculated from the slopes and intercepts, respectively, by plotting Van't Hoff's plot between ln K_d and 1000/T (Fig. 16). The value of Gibb's free energy $\Delta G°$ (kJ/mol) was calculated using Eqs. 10 and 11. The results of the thermodynamic study are presented in

Table 3. The negative value of enthalpy change (ΔH°) signifies that the process is an exothermic type and the amount of adsorption involves the formation of certain chemical processes that are present throughout the adsorption process (Kumar et al. 2013). The negative value of free energy change (ΔG°) proves that the adsorption process is spontaneous and feasible at a given temperature. The decreasing value of ΔG° with increase in temperature depicts that the degree of feasibility decreases for Cr^{6+} adsorption. The negative value of ΔH° and ΔS° indicates that the process is spontaneous at low temperature and non-spontaneous at a higher temperature. It was observed that the adsorption process was exothermic and spontaneous.

Comparative study of adsorbent

A comparison of maximum adsorption capacity data of various aquatic plants that have been used by various investigators for the adsorption of Cr^{6+} is listed in Table 4. Various aquatic plants like *Lepironia articulate* (Kaewsichan and

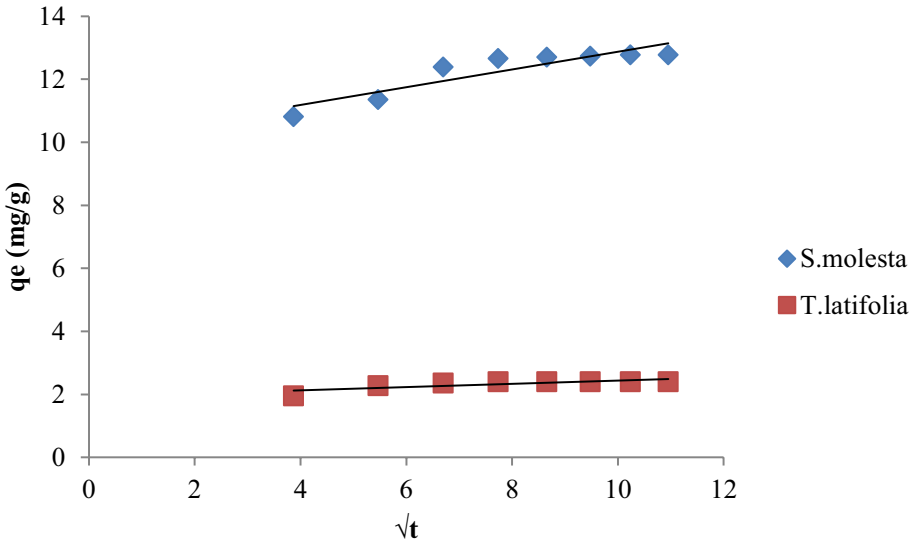

Fig. 15 Intraparticle diffusion plot for Cr^{6+} adsorption on *S. molesta* and *T. Latifolia*

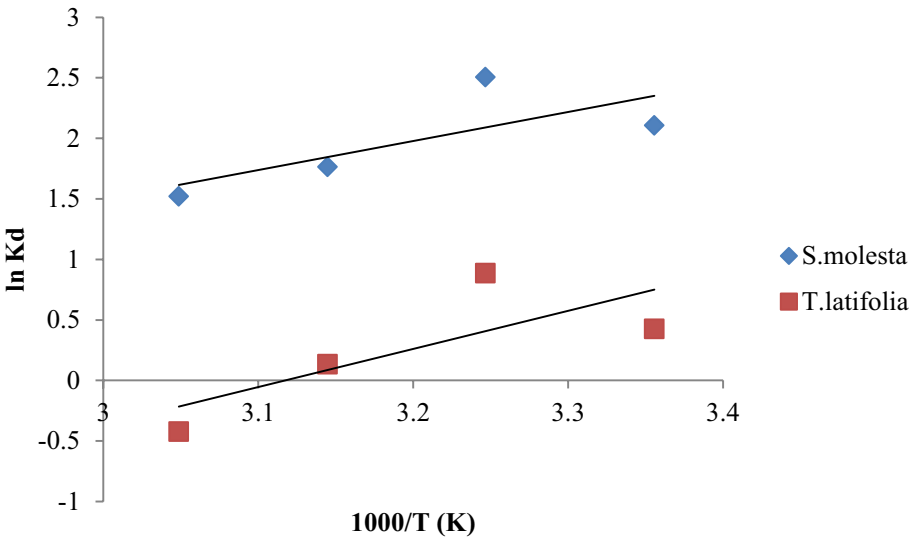

Fig. 16 Van't Hoff's plot for Cr^{6+} adsorption on *S. molesta* and *T. latifolias*

Table 3 Thermodynamic parameters for adsorption of Cr^{6+} on *S. molesta* and *T. latifolia*

Adsorbent	ΔH° (kJ/mol)	ΔS° (kJ/K. mol)	ΔG° (kJ/mol)			
			298 K	308 K	318 K	328 K
molesta	–19.93	–0.047	–5.93	–5.46	–4.99	–4.52
latifolia	–26.18	–0.08	–2.34	–1.54	–0.74	0.06

Table 4 Various aquatic plant adsorbents with their adsorption capacities and experimental conditions

Adsorbent	Metal adsorbed	pH	Dose (g)	Conc. (mg/L)	Time (min)	Temp. (°C)	Monolayer adsorption capacity, q_m (mg/g)	References
Lepironia articulate	Cr^{6+}	2	0.3	50	100	60	21.90	(Kaewsichan and Tohdee 2019)
Pistia stratiotes	Cr^{6+}	2	0.25	10	15	40	7.24	(Das et al. 2013)
Azolla filiculoides	Cr^{6+}	2	0.5	20	100	30	10.63	(Babu et al. 2014)
Hydrilla verticillata	Cr^{6+}	4.5	2.5	10	80	30	29.43	(Mishra et al. 2014)
Eichhornia crassipes	Cr^{6+}	3	0.5	10	120	25	7.50	(Gude and Das 2008)
Salvinia molesta	Cr^{6+}	1	0.15	20	60	25	33.33	Present study
Typha latifolia	Cr^{6+}	1	0.8	20	60	25	10.30	Present study

Tohdee 2019), *Pistia stratiotes* (Das et al. 2013), *Azolla filiculoides* (Babu et al. 2014), *Hydrilla verticillata* (Mishra et al. 2014), and *Eichhornia crassipes* (Gude and Das 2008) have been used for removal of Cr^{6+}. The maximum reported adsorption capacities of these plants were 21.90, 7.24, 10.63, 29.43, and 7.5 mg/g, respectively.

Conclusion

In this study, aquatic plants *S. molesta* and *T. latifolia* were used as adsorbents to study their potential to adsorb Cr^{6+}. Characterization studies (SEM and FTIR) showed the structural and morphological details of the adsorbent. Adsorption was found to be pH dependent, and monolayer adsorption capacity was found to be 33.33 and 10.30 mg/g for *S. molesta* and *T. latifolia*, respectively, at pH 1, 20 mg/L, a contact time of 60 min, 150 rpm, 25 °C and dose of 0.150 g (*S. molesta*) and 0.8 g (*T. latifolia*). Adsorption isotherm model revealed that Langmuir isotherm was fitted for *S. molesta* and Freundlich isotherm fitted with *T. latifolia* adsorption data. The pseudo-second-order kinetic was fitted well to both the adsorbents. The thermodynamic study showed that the adsorption process was exothermic and spontaneous. Overall, both aquatic plants were found to be good adsorbents for Cr^{6+} removal. These adsorbents can be used for the removal of other metals also. Furthermore, the adsorption efficiency of these adsorbents can be increased by modifying with acid, base, and other chemical species.

Acknowledgements The authors are thankful to Dr Surender Yadav, Department of Botany, M.D. University for identification of aquatic plant species.

Authors contribution Asha Singh was involved in conceptualization, data curation, writing original draft, and editing; Sunil Kumar helped in supervision and editing; Vishal Panghal helped in visualization and editing.

Funding The author(s) received no specific funding for this work.

Declarations

Conflict of interest The authors declare that they have no conflict of interest.

Consent to participate Not Applicable.

Consent to publish Not Applicable.

Availability of data and materials Nil.

References

Afroze S, Sen T, Ang M (2015) Agricultural solid wastes in aqueous phase dye adsorption: a review. In: Agricultural wastes: Characteristics, types and management. Nova Publishers, pp 169–213

Afroze S, Sen TK (2018) A review on heavy metal ions and dye adsorption from water by agricultural solid waste adsorbents. Water Air Soil Pollut 229(7):225

Ahluwalia SS, Goyal D (2007) Microbial and plant derived biomass for removal of heavy metals from wastewater. Bioresour Technol 98(12):2243–2257

Ahmad R, Haseeb S (2015) Black cumin seed (BCS): a non conventional adsorbent for the removal of Cu (II) from aqueous solution. Desalin Water Treat 56(9):2512–2521

Ali A, Saeed K, Mabood F (2016) Removal of chromium (VI) from aqueous medium using chemically modified banana peels as efficient low-cost adsorbent. Alexandria Eng J 55(3):2933–2942
Al-Senani GM, Al-Fawzan FF (2018) Adsorption study of heavy metal ions from aqueous solution by nanoparticle of wild herbs. Egyptian J Aquatic Res 44(3):187–194
APHA (1985) Standard methods for the examination of water and wastewater, 16th edn APHA, AWWA, WPCF, Washington
Babu BV, Gupta S (2008) Adsorption of Cr (VI) using activated neem leaves: kinetic studies. Adsorption 14(1):85–92
Babu DJ, Sumalatha B, Venkateswarulu TC, Das KM, Kodali VP (2014) Kinetic, equilibrium and thermodynamic studies of biosorption of Chromium (VI) from aqueous solutions using Azolla Filiculoidus. J Pure Appl Microbio 8(4):3107–3116
Balasubramanian UM, Murugaiyan SV, Marimuthu T (2019) Enhanced adsorption of Cr (VI), Ni (II) ions from aqueous solution using modified Eichhornia crassipes and Lemna minor. Environ Sci Pollut Res 1–15
Bayat B (2002) Comparative study of adsorption properties of Turkish fly ashes: I. The case of nickel (II), copper (II) and zinc (II). J Hazard Mater 95(3):251–273
Bind A, Goswami L, Prakash V (2018) Comparative analysis of floating and submerged macrophytes for heavy metal (copper, chromium, arsenic and lead) removal: sorbent preparation, characterization, regeneration and cost estimation. Geology Ecology and Landscapes 2(2):61–72
Borah L, Senapati KK, Borgohain C, Sarma S, Roy S, Phukan P (2012) Preparation of ordered porous carbon from tea by chemical activation and its use in Cr (VI) adsorption. J Porous Mater 19(5):767–774
Chen JP, Hong L, Wu S, Wang L (2002) Elucidation of interactions between metal ions and Ca alginate-based ion-exchange resin by spectroscopic analysis and modeling simulation. Langmuir 18(24):9413–9421
Das B, Mondal NK, Chattaraj PRS (2013) Equilibrium, kinetic and thermodynamic study on chromium (VI) removal from aqueous solution using Pistia stratiotes biomass. Chem Sci Trans 2(1):85–104
Feng LF, Qi W (2011) Removal of heavy metal ions from wastewaters. J Environ Mgmt 92(3):407–418
Flores-Cano JV, Leyva-Ramos R, Carrasco-Marin F, Aragón-Piña A, Salazar-Rabago JJ, Leyva-Ramos S (2016) Adsorption mechanism of Chromium (III) from water solution on bone char: effect of operating conditions. Adsorption 22(3):297–308
Freundlich HMF (1906) Over the adsorption in solution. J Phys Chem 57(385471):1100–1107
Goswami M, Borah L, Mahanta D, Phukan P (2014) Equilibrium modeling, kinetic and thermodynamic studies on the adsorption of Cr (VI) using activated carbon derived from matured tea leaves. J Porous Mater 21(6):1025–1034
Grimshaw P, Calo JM, Hradil G (2011) Cyclic electrowinning/precipitation (CEP) system for the removal of heavy metal mixtures from aqueous solutions. Chem Eng J 175:103–109
Gude SM, Das SN (2008) Adsorption of chromium (VI) from aqueous solutions by chemically treated water hyacinth Eichhornia crassipes. Ind J Chem Technol 15:12–18
Gupta S, Babu BV (2009) Removal of toxic metal Cr (VI) from aqueous solutions using sawdust as adsorbent: Equilibrium, kinetics and regeneration studies. Chem Eng J 150(2–3):352–365
Hanafiah MAKM, Zakaria H, Ngah WW (2009) Preparation, characterization, and adsorption behavior of Cu (II) ions onto alkali-treated weed (Imperata cylindrica) leaf powder. Water Air Soil Pollut 201(1–4):43–53
Hashem MA, Hasan M, Momen MA, Payel S, Nur-A-Tomal MS (2020) Water hyacinth biochar for trivalent chromium adsorption from tannery wastewater. Environ Sustainability Indicators 5:100022
Hassoon HA, Najem AM (2017) Removal of some traces heavy metals from aqueous solutions by water Hyacinth leaves powder. Iraqi J Sci 58(2A):611–618
Jain M, Garg VK, Kadirvelu K (2009) Equilibrium and kinetic studies for sequestration of Cr (VI) from simulated wastewater using sunflower waste biomass. J Hazard Mater 171(1–3):328–334
Jain M, Garg VK, Kadirvelu K (2010) Adsorption of hexavalent chromium from aqueous medium onto carbonaceous adsorbents prepared from waste biomass. J Environ Mgmt 91(4):949–957
Jianlong W, Xinmin Z, Yi Q (2000) Removal of Cr (VI) from aqueous solution by macroporous resin adsorption. J Environ Sci Health Part A 35(7):1211–1230
Kaewsichan L, Tohdee K (2019) Adsorption of hexavalent chromium onto alkali-modified biochar derived from Lepironia articulata: a kinetic, equilibrium, and thermodynamic study. Water Env Res 91(11):1433–1446
Kratochvil D, Volesky B (1998) Advances in the biosorption of heavy metals. Trends Biotechnol 16(7):291–300
Kumar M, Tamilarasan R, Sivakumar V (2013) Adsorption of Victoria blue by carbon/Ba/alginate beads: kinetics, thermodynamics and isotherm studies. Carbohyd Polym 98(1):505–513
Lagergren SK (1898) About the theory of so-called adsorption of soluble substances. Sven Vetenskapsakad Handingarl 24:1–39
Langmuir I (1918) The adsorption of gases on plane surfaces of glass, mica and platinum. J Am Chem Soc 40(9):1361–1403
Li Q, Chen B, Lin P, Zhou J, Zhan J, Shen Q, Pan X (2016) Adsorption of heavy metal from aqueous solution by dehydrated root powder of long-root Eichhornia crassipes. Int J Phytoremed 18(2):103–109
Lima LK, Pelosi BT, da Silva MGC, Vieira MG (2013) Lead and chromium biosorption by Pistia stratiotes biomass. Chem Eng Trans 32:1045–1050
Liu Y, Yan J, Yuan D, Li Q, Wu X (2013) The study of lead removal from aqueous solution using an electrochemical method with a stainless steel net electrode coated with single wall carbon nanotubes. Chem Eng J 218:81–88
Llanos J, Camarillo R, Pérez Á, Cañizares P (2010) Polymer supported ultrafiltration as a technique for selective heavy metal separation and complex formation constants prediction. Sep Purif Technol 73(2):126–134
Loganathan P, Shim WG, Sounthararajah DP, Kalaruban M, Nur T, Vigneswaran S (2018) Modelling equilibrium adsorption of single, binary, and ternary combinations of Cu, Pb, and Zn onto granular activated carbon. Environ Sci Pollut Res 25(17):16664–16675
Meitei MD, Prasad MNV (2014) Adsorption of Cu (II), Mn (II) and Zn (II) by Spirodela polyrhiza (L.) Schleiden: equilibrium, kinetic and thermodynamic studies. Ecol Eng 71:308–317
Mishra A, Tripathi BD, Rai AK (2014) Biosorption of Cr (VI) and Ni (II) onto Hydrilla verticillata dried biomass. Ecol Eng 73:713–723
Mohanty K, Jha M, Meikap BC, Biswas MN (2006) Biosorption of Cr (VI) from aqueous solutions by Eichhornia crassipes. Chem Eng J 117(1):71–77
Musico YLF, Santos CM, Dalida MLP, Rodrigues DF (2013) Improved removal of lead (II) from water using a polymer-based graphene oxide nanocomposite. J Mater Chem A 1(11):3789–3796
Ngah WW, Hanafiah MAKM (2008) Adsorption of copper on rubber (Hevea brasiliensis) leaf powder: Kinetic, equilibrium and thermodynamic studies. Biochem Eng J 39(3):521–530
Oehmen A, Viegas R, Velizarov S, Reis MA, Crespo JG (2006) Removal of heavy metals from drinking water supplies through the ion exchange membrane bioreactor. Desalination 199(1–3):405–407
Patel S (2012) Threats, management and envisaged utilizations of aquatic weed Eichhornia crassipes: an overview. Reviews Environ Sci Bio/technol 11(3):249–259

Rajaei GE, Aghaie H, Zare K, Aghaie M (2013) Adsorption of Cu (II) and Zn (II) ions from aqueous solutions onto fine powder of Typha latifolia L. root: kinetics and isotherm studies. Res Chem Intermed 39(8):3579–3594

Raji C, Anirudhan TS (1998) Batch Cr (VI) removal by polyacrylamide-grafted sawdust: kinetics and thermodynamics. Water Res 32(12):3772–3780

Sankaran NB, Anirudhan TS (1999) Adsorption dynamics of phenol on activated carbon produced from Salvinia molesta Mitchell by single-step steam pyrolysis. Indian J Eng Mater Sci 6:229–236

Saraswat S, Rai JPN (2010) Heavy metal adsorption from aqueous solution using Eichhornia crassipes dead biomass. Int J Mineral Processing 94(3–4):203–206

Sharma PK, Ayub S, Tripathi CN (2016) Isotherms describing physical adsorption of Cr (VI) from aqueous solution using various agricultural wastes as adsorbents. Cogent Eng 3(1):1186857

Singh A, Kumar S, Panghal V, Arya SS (2019) Utilization of unwanted terrestrial weeds for removal of dyes. Rasayan J Chem 12(4):1956–1963

Singh R, Bhateria R (2020) Experimental and modeling process optimization of lead adsorption on magnetite nanoparticles via isothermal, kinetics, and thermodynamic studies. ACS Omega 5:10826–10837

Soni H, Padmaja P (2014) Palm shell based activated carbon for removal of bisphenol A: an equilibrium, kinetic and thermodynamic study. J Porous Mater 21(3):275–284

Temkin MJ, Pyzhev V (1940) Recent modifications to Langmuir isotherms.

Tewari N, Vasudevan P, Guha BK (2005) Study on biosorption of Cr (VI) by Mucor hiemalis. Biochem Eng J 23(2):185–192

Thitame PV, Shukla SR (2017) Removal of lead (II) from synthetic solution and industry wastewater using almond shell activated carbon. Environ Prog Sustain Energy 36(6):1628–1633

Tolcha T, Gemechu T, Megersa N (2020) Flower of Typha latifolia as a low-cost adsorbent for quantitative uptake of multiclass pesticide residues from contaminated waters. South Afr J Chem 73:22–29

Wanees SA, Ahmed AMM, Adam MS, Mohamed MA (2013) Adsorption studies on the removal of hexavalent chromium-contaminated wastewater using activated carbon and bentonite. Asian J Chem 25(15):8245–8252

Wang XS, Tang YP, Tao SR (2008) Removal of Cr (VI) from aqueous solutions by the nonliving biomass of alligator weed: Kinetics and equilibrium. Adsorption 14(6):823

Weber WJ, Morris JC (1963) Kinetics of adsorption on carbon from solution. J Sanitary Eng Div 89(2):31–60

Weis JS, Weis P (2004) Metal uptake, transport and release by wetland plants: implications for phytoremediation and restoration. Environ Int 30:685–700

Wittbrodt PR, Palmer CD (1995) Reduction of Cr (VI) in the presence of excess soil fulvic acid. Environ Sci Technol 29(1):255–263

Ys H, Mckay G, Ys H, Mckay G (1999) Pseudo-second order model for sorption processes. Process Biochem 34(5):451–465